

## Limiting blazar redshifts through extragalactic background light attenuation

María Láinez,<sup>a,\*</sup> Alberto Domínguez,<sup>a</sup> Vaidehi S. Paliya,<sup>b</sup> Nuria Álvarez-Crespo,<sup>a</sup> Marco Ajello,<sup>c</sup> Justin Finke,<sup>d</sup> Mireia Nievas-Rosillo,<sup>e,f</sup> Jose Luis Contreras<sup>a</sup> and Abhishek Desai<sup>g</sup>

<sup>a</sup>IPARCOS and Department of EMFTEL, Universidad Complutense de Madrid, E-28040 Madrid, Spain

<sup>b</sup>Inter-University Centre for Astronomy and Astrophysics (IUCAA), SPPU Campus, 411007, Pune, India

<sup>c</sup>Department of Physics and Astronomy, Clemson University, Kinard Lab of Physics, Clemson, SC 29634-0978, US

<sup>d</sup>U.S. Naval Research Laboratory, Code 7653, 4555 Overlook Avenue SW, Washington, DC 20375-5352, USA

<sup>e</sup>Instituto de Astrofísica de Canarias, E-38205 La Laguna, Tenerife, Spain

<sup>f</sup>Universidad de La Laguna, Dept. Astrofísica, E-38206 La Laguna, Tenerife, Spain

<sup>g</sup>Department of Physics and Wisconsin IceCube Particle Astrophysics Center, University of Wisconsin-Madison, Madison, WI 53706, USA

E-mail: [malainez@ucm.es](mailto:malainez@ucm.es), [alberto.d@ucm.es](mailto:alberto.d@ucm.es)

The high-energy gamma-ray sky is dominated by blazars, active galactic nuclei with their jets pointing towards us. Measuring distances to these sources is challenging because any spectral signature from the galaxy may be outshone by the non-thermal emission from the jet. In this contribution, we present a method to constrain redshifts for these sources that relies only on data from the Large Area Telescope on board the *Fermi Gamma-ray Space Telescope*. This method takes advantage of signatures that arise in gamma-ray spectra and result from pair-production interactions between photons with energies larger than approximately 10 GeV and the extragalactic background light. We find upper limits to the distances to 303 gamma-ray blazars that previously did not have redshifts, including 157 BL Lacertae objects, 145 of uncertain class, and 1 flat-spectrum-radio quasar, whose redshift is otherwise unknown. These derivations can be useful for planning observations with Imaging Atmospheric Cherenkov Telescopes and also for testing theories of supermassive black hole evolution. Our results are applied for estimating the detectability of these blazars with the MAGIC telescopes, finding that at least 4 of them could be studied in a reasonable exposure of 20 hours.

38th International Cosmic Ray Conference (ICRC2023)  
26 July - 3 August, 2023  
Nagoya, Japan



---

\*Speaker

## 1. Introduction

Blazars are active galactic nuclei (AGNs) with their jets pointing towards us. These are the most numerous type of extragalactic sources detected at high-energy (HE,  $100 \text{ MeV} < E < 100 \text{ GeV}$ ) and very-high-energy (VHE,  $E > 100 \text{ GeV}$ ) gamma rays. They can be classified in two main groups based on the presence or absence of emission lines in their optical spectra, with flat-spectrum-radio quasars (FSRQs) being characterized by the presence of broad emission lines and the opposite for BL Lacerate objects (BL Lacs). The absence of strong emission lines in the spectra of BL Lacs makes it difficult to constrain the distance at which they are located. For this reason, the redshifts of many of these sources remain unknown. In fact, roughly 50% of the blazars in the 4FGL catalogue do not have redshift measurements [1, 2].

Determining the distances to blazars is essential to study their evolution and emission mechanisms. This has led to the development of new methodologies to estimate their redshifts which are not based on optical spectral measurements, such as the use of the attenuation by the extragalactic background light (EBL) [3–5]. The EBL, that is the accumulated radiation produced by star formation processes throughout the history of the universe, leaves an imprint in the HE gamma-ray spectra of blazars that can be used to determine the distances at which they are located. The pair-production interaction of EBL photons with gamma rays emitted by AGNs leads to an optical depth,  $\tau(E, z)$ , that depends on the energy of the gamma-ray photons and the redshift of the emitting source. This optical depth is responsible for attenuation in the  $E > 10 \text{ GeV}$  gamma-ray spectra of blazars [e.g., 6, 7]. In this contribution, we present a new methodology to estimate the redshifts of blazars using gamma-ray data taken by the Large Area Telescope (LAT) on board the *Fermi Gamma-ray Space Telescope* and the attenuation generated by the EBL.

## 2. Sample selection and data analysis

For our analysis, we first select all blazars in the 4FGL-DR2 catalogue [8]. These correspond to (non-variable/variable blazars) 621/510 BL Lacs, 866/446 blazar candidates of uncertain type (BCUs), and 129/565 FSRQs. The sources are classified as variable or non-variable depending on whether the `Variability_Index` value given in 4FGL-DR2 is higher or lower than 18.48, as explained in [9]. For each of these sources we perform a likelihood analysis using the *Fermi*-LAT spectral data given in the 4FGL-DR2 catalogue and following the next steps:

1. We perform a likelihood analysis in the 1 GeV - 2 TeV range assuming there is no EBL ( $\tau = 0$ ) and we extract the spectral parameters of all the sources lying in our region of interest (ROI, 7 deg) plus a radius R (3 deg).
2. We perform a likelihood analysis in the 1 GeV - 10 GeV energy range, freezing all the values of the spectral parameters to those obtained in the previous step, except for our source of interest. The EBL is also not considered in this step, since the EBL absorption is not significant at energies below 10 GeV. Thus, this step allows us to determine the intrinsic gamma-ray spectrum of the considered source.
3. We extrapolate the spectral shape obtained in step (2) to the 10 GeV - 2 TeV range and add the EBL attenuation. The absorption due to the EBL is added as an exponential term in the optical

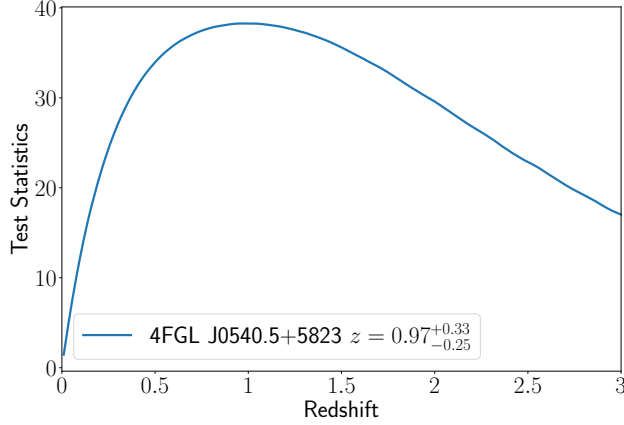


**Figure 1:** Example of the TS profile obtained for one of the blazars of our sample, 4FGL J0540.5+5823, showing the TS obtained in our analysis for each redshift value considered (from 0.01 to 3 in steps of 100).

depth,  $\exp[-\tau(E, z)]$ . We perform the analysis for different values of the redshift, going from 0.01 to 3 in steps of 100, and for each of these redshifts we extract the log-likelihood value of the analysis performed.

4. We create a Test Statistics (TS) profile for each of the sources of our sample by comparing the log-likelihood value obtained in step (3) with the one derived in step (1), obtaining a profile such as the one given in Fig. 1. The TS is defined as  $TS = 2 \log(L_1 - L_0)$ , where  $L_0$  is the likelihood value of the null hypothesis (i.e. no EBL absorption) and  $L_1$  is the likelihood value of the alternative hypothesis (i.e. EBL absorbed spectrum at the considered redshift). The maximum-likelihood value of the redshift for the considered source is that corresponding to the peak of the TS profile,  $TS_{\text{peak}}$ . The redshift obtained with this method should be interpreted as an upper limit, since the gamma-ray spectra of the blazars could have an intrinsic curvature that is not due to the EBL attenuation.

After performing the analysis for all the sources in 4FGL-DR2, we select only those for which  $TS_{\text{peak}} \geq 1$ , and for which the TS profile shows a peak for  $z \leq 3$ . This leaves us with 344/331 non-variable/variable blazars in our sample: 5/40 FSRQs, all of them with redshift in the 4LAC catalogue [1], except 4FGL J1532.7-1319; and 338/293 blazars classified as BL Lacs or BCUs, of which 172/130 do not have a redshift in 4LAC. Thus, we have obtained estimates for the redshifts of 303 gamma-ray blazars that previously had an unknown redshift.

### 3. Results and discussion

#### 3.1 Estimates of the redshift of blazars

In order to demonstrate that our methodology gives reliable results, we compute the EBL redshift of all blazars with redshift in 4FGL-DR2 that fulfill the conditions explained in the previous section ( $TS_{\text{peak}} \geq 1$  and TS profile showing a peak in  $z \leq 3$ ). We then compare the resulting redshift values with the ones given in 4LAC. Figure 2 shows the EBL redshift obtained here versus the one

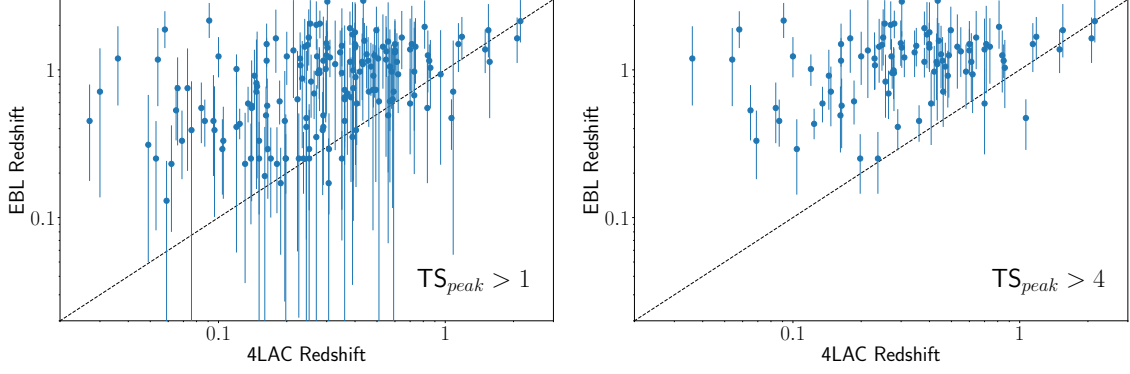


**Figure 2:** Comparison of the redshift obtained with our methodology using the EBL attenuation with that given in the 4LAC catalogue for the non-variable sources of our sample that have a redshift in 4LAC, and  $TS_{\text{peak}} \geq 1$  (166 sources, left) and  $TS_{\text{peak}} \geq 4$  (91 sources, right).

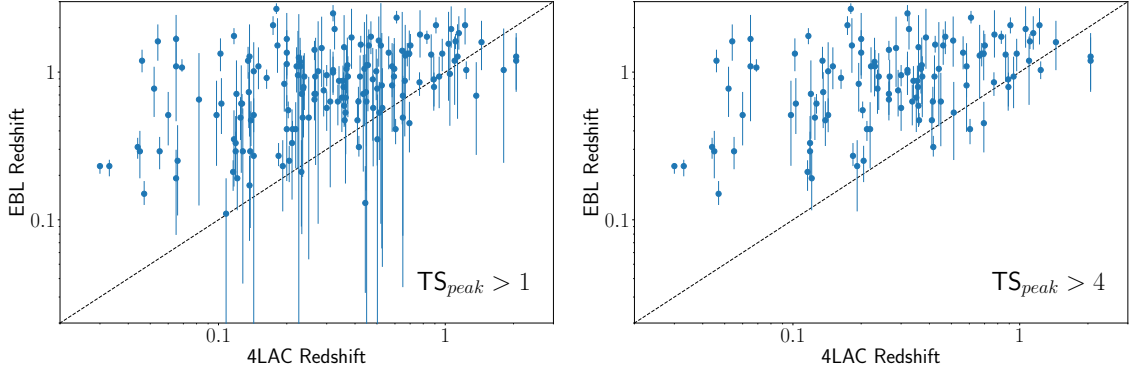


**Figure 3:** Comparison of the redshift obtained with our methodology using the EBL attenuation with that given in the 4LAC catalogue for the variable sources of our sample that have a redshift in 4LAC, and  $TS_{\text{peak}} \geq 1$  (162 sources, left) and  $TS_{\text{peak}} \geq 4$  (111 sources, right).

given in 4LAC for the 166 non-variable sources of the sample with  $TS_{\text{peak}} \geq 1$  and for the 91 non-variable sources with  $TS_{\text{peak}} \geq 4$ . Figure 3 shows the same comparison plot for the 162 variable sources with  $TS_{\text{peak}} \geq 1$  and for the 111 variable sources with  $TS_{\text{peak}} \geq 4$ . These figures show that the redshifts obtained here can, indeed, be interpreted as upper limits, both for variable and non-variable sources.

For the variable sources, it has been tested that the resulting redshift values are different for distinct time periods. However, in most cases the resulting redshift is still an upper limit. For a detailed study and discussion of the sources that lie below the one-to-one line in Figures 2 and 3, see [10].

The redshift estimates derived here for the 303 selected blazars with previously unknown redshift can be found in Table 1 of [10]. The photon index of all these sources as a function of their flux above 10 GeV is shown in Figure 4, and compared with all the sources from 4FGL-DR2 catalogue. As expected, the blazars for which we could estimate the redshift with the methodology explained above (i.e. the analysis gave a  $TS_{\text{peak}} \geq 1$  and the TS profile peaked for  $z \leq 3$ ) are located in the lower part of the diagram, meaning that they correspond to blazars with hard spectra, i.e. low

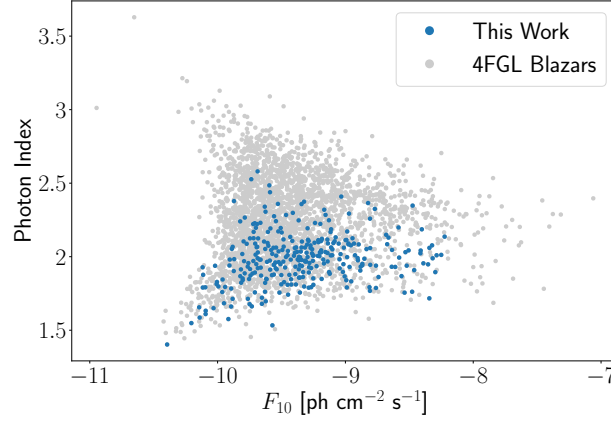


**Figure 4:** Photon index given in 4FGL as a function of the integrated flux above 10 GeV for all the blazars in the 4FGL-DR2 catalogue (in grey) and for the blazars selected here for the estimation of their redshift (in blue).

photon index.

### 3.2 Application of the obtained redshift estimates to make detectability predictions

As a possible application case of the obtained redshift estimates, we check the detectability predictions with the MAGIC telescopes of some gamma-ray blazars of our sample using the estimated redshifts. In particular, for this study, we select all the blazars of the sample that can be observed with a zenith angle  $\leq 45$  deg from the MAGIC site.

The Crab Nebula and background rates given in [11] are used for the estimation of the expected detection significance of the blazars with MAGIC. These rates are given for two different zenith angle ranges, 0-30 deg and 30-45 deg. We assume observations around culmination time to determine the zenith angle at which each source could be observed, and classify our sources in the two different zenith angle ranges to employ the corresponding Crab Nebula and background rates. These rates are used to derive the expected number of excess and off events that would be observed from the considered source in 20 hours. The total number of background events in each energy bin is calculated as the background rate times the considered observation time, i.e. 20 hours in this case. The number of excess events is obtained by scaling linearly the flux of our source with that of the Crab Nebula in each energy bin, and then multiplying by the Crab Nebula rate and observation time. The number of excess and background events are finally used to compute the statistical detection significance of each source.

The spectral shape of the source is assumed to be the one obtained in our LAT data analysis for the redshift calculation, which is a PowerLaw or a LogParabola. This spectral shape is extrapolated to TeV energies and the EBL absorption is applied using the optical depth values given in [12], based on the EBL model by Saldana-López et al. [13]. For the source redshifts used in estimating the expected detection significances, we use the 68% upper confidence interval values for the  $\text{TS}_{\text{peak}}$  values given in Table 1 of [10].

From the 303 blazars in our sample, there are 180 that can be observed with a zenith angle  $\leq 45$  deg from the MAGIC site, from which 3 give an expected detection significance  $> 5 \sigma$  with

4FGL Source Name	Redshift Upper Limit	$TS_{peak}$	HEP (GeV)	Type	Association	TeV	MAGIC ( $\sigma$ )
J0035.9+5950	$1.03^{+0.08}_{-0.10}$	739.82	373	bll	1ES 0033+595	Y	5.6
J0136.5+3906	$0.73^{+0.13}_{-0.12}$	35.07	251	bll	B3 0133+388	Y	4.4
J1942.7+1033	$0.55^{+0.12}_{-0.12}$	35.58	181	bll	87GB 194024.3+102612	N	6.0
J2056.7+4939	$0.17^{+0.06}_{-0.08}$	6.39	310	bcu	RGB J2056+496	Y	11.5

**Table 1:** Main information of the 4 sources for which we get an expected detection significance  $> 5\sigma$  with MAGIC in 20 hours. The information shown is: name of the source in the 4FGL catalogue, redshift upper limit derived from our EBL-attenuation methodology (uncertainties are at 68% C.L.), value of the peak of the TS profile, highest energy photon, source type (bll is BL Lac and bcu is blazar candidate of uncertain type), source association, whether the source is detected by IACTs (Yes or No), and predicted detection significance with MAGIC in 20 hours.

MAGIC in 20 hours. If we take the redshifts at the  $TS_{peak}$  values, we get an additional candidate to be detected by MAGIC. The results for these 4 sources are shown in Table 1, where the listed significances are obtained using the upper limit value of the redshift. Out of these candidates, 3 of them have already been detected at TeV energies. In fact, 4FGL J0035.9+5950 and 4FGL J0136.5+3906 were detected by MAGIC [14, 15], while 4FGL J2056.7+4939 was detected by VERITAS [16]. 4FGL J1942.7+1033 has yet to be detected in VHE gamma rays, although our results show that it could be a good target for IACTs.

#### 4. Summary and Conclusions

We have obtained estimates for the redshifts of 303 gamma-ray blazars that previously did not have redshift measurements, employing a new methodology that uses solely *Fermi*-LAT data and the EBL absorption. Most of these blazars are BL Lacs, for which the determination of the redshift is more challenging due to the lack of emission lines in their spectra. Determining blazar redshifts is necessary in order to understand their evolution and their emission mechanisms, as well as to be able to plan observations with IACTs. In fact, these new redshifts have allowed us to calculate the detectability of these blazars with the MAGIC telescopes, finding that at least 4 of them could be detected with an exposure of 20 hours.

#### Acknowledgements

The *Fermi*-LAT Collaboration acknowledges support for LAT development, operation and data analysis from NASA and DOE (United States), CEA/Irfu and IN2P3/CNRS (France), ASI and INFN (Italy), MEXT, KEK, and JAXA (Japan), and the K.A. Wallenberg Foundation, the Swedish Research Council and the National Space Board (Sweden). Science analysis support in the operations phase from INAF (Italy) and CNES (France) is also gratefully acknowledged. This work performed in part under DOE Contract DE-AC02-76SF00515.

A.D. is thankful for the support of the Ramón y Cajal program from the Spanish MINECO, Proyecto PID2021-126536OA-I00 funded by MCIN / AEI / 10.13039/501100011033, and project PR44/21-29915 funded by the Santander Bank and Universidad Complutense de Madrid. M.L. is

funded by MCIN through grant PRE2020-093502. J.L.C. is supported by MCIN project PID2019-104114RB-C32. J.F. is partially supported by NASA through contract S-15633Y.

## References

- [1] M. Ajello, R. Angioni, M. Axelsson, J. Ballet, G. Barbiellini, D. Bastieri et al., *The Fourth Catalog of Active Galactic Nuclei Detected by the Fermi Large Area Telescope*, *The Astrophysical Journal* **892** (2020) 105 [1905.10771].
- [2] S. Abdollahi, F. Acero, L. Baldini, J. Ballet, D. Bastieri, R. Bellazzini et al., *Incremental Fermi Large Area Telescope Fourth Source Catalog*, *The Astrophysical Journal Supplement Series* **260** (2022) 53 [2201.11184].
- [3] E. Prandini, G. Bonnoli, L. Maraschi, M. Mariotti and F. Tavecchio, *Constraining blazar distances with combined Fermi and TeV data: an empirical approach*, *Monthly Notices of the Royal Astronomical Society* **405** (2010) L76 [1003.1674].
- [4] J. Yang and J. Wang, *Redshifts of Distant Blazars Limited by Fermi and VHE  $\gamma$ -Ray Observations*, *Publications of the Astronomical Society of Japan* **62** (2010) L23 [1006.4401].
- [5] V.A. Acciari, T. Aniello, S. Ansoldi, L.A. Antonelli, A. Arbet Engels, C. Arcaro et al., *Long-term multi-wavelength study of IES 0647+250*, *A&A* **670** (2023) A49 [2211.13268].
- [6] M. Ackermann, M. Ajello, A. Allafort, P. Schady, L. Baldini, J. Ballet et al., *The imprint of the extragalactic background light in the gamma-ray spectra of blazars.*, *Science* **338** (2012) 1190 [1211.1671].
- [7] S. Abdollahi, M. Ackermann, M. Ajello, W.B. Atwood, L. Baldini, J. Ballet et al., *A gamma-ray determination of the Universe's star formation history*, *Science* **362** (2018) 1031 [1812.01031].
- [8] J. Ballet, T.H. Burnett, S.W. Digel and B. Lott, *Fermi Large Area Telescope Fourth Source Catalog Data Release 2*, *arXiv e-prints* (2020) arXiv:2005.11208 [2005.11208].
- [9] S. Abdollahi, F. Acero, M. Ackermann, M. Ajello, W.B. Atwood, M. Axelsson et al., *Fermi Large Area Telescope Fourth Source Catalog*, *The Astrophysical Journal Supplement Series* **247** (2020) 33 [1902.10045].
- [10] A. Domínguez, M. Láinez, V.S. Paliya, N. Álvarez-Crespo, M. Ajello, J. Finke et al., *Constraints on redshifts of blazars from extragalactic background light attenuation using Fermi-LAT data*, *arXiv e-prints* (2023) arXiv:2307.10083 [2307.10083].
- [11] J. Aleksić, S. Ansoldi, L.A. Antonelli, P. Antoranz, A. Babic, P. Bangale et al., *The major upgrade of the MAGIC telescopes, Part II: A performance study using observations of the Crab Nebula*, *Astroparticle Physics* **72** (2016) 76.

- [12] A. Domínguez, P. Østergaard Kirkeberg, R. Wojtak, A. Saldana-Lopez, A. Desai, J. Primack et al., *A new derivation of the Hubble constant from  $\gamma$ -ray attenuation using improved optical depths for the Fermi and CTA era*, *arXiv preprint arXiv:2306.09878* (2023) .
- [13] A. Saldana-Lopez, A. Domínguez, P.G. Pérez-González, J. Finke, M. Ajello, J.R. Primack et al., *An observational determination of the evolving extragalactic background light from the multiwavelength HST/CANDELS survey in the Fermi and CTA era*, *Monthly Notices of the Royal Astronomical Society* **507** (2021) 5144 [2012.03035].
- [14] M. Mariotti et al., *VHE detection of the blazar 1ES 0033+ 595 by MAGIC*, *The Astronomer's Telegram* **3719** (2011) 1.
- [15] K. Nilsson, T. Pursimo, C. Villforth, E. Lindfors, L.O. Takalo and A. Sillanpää, *Redshift constraints for RGB 0136+391 and PKS 0735+178 from deep optical imaging*, *A&A* **547** (2012) A1 [1209.4755].
- [16] R. Mukherjee et al., *VERITAS Discovery of VHE Emission from RGB J2056+ 496*, *The Astronomer's Telegram* **9721** (2016) 1.